THE JOURNAL OF BIOLOGICAL CHEMISTRY VOL. 286, NO. 44, pp. 38714–38724, November 4, 2011

Characterization and Scope of S-layer Protein *O*-Glycosylation in *Tannerella forsythia*[*] [S]

Received for publication, July 6, 2011, and in revised form, August 29, 2011 Published, JBC Papers in Press, September 9, 2011, DOI 10.1074/jbc.M111.284893

Gerald Posch[‡1], **Martin Pabst**[§1], **Lothar Brecker**[¶], **Friedrich Altmann**[§], **Paul Messner**[‡], **and Christina Schäffer**[‡2]

From the [‡]*Department of NanoBiotechnology, NanoGlycobiology, Vienna Institute of BioTechnology, Universität für Bodenkultur Wien, Muthgasse 11, A-1190 Vienna, Austria, the* [§]*Department of Chemistry, Vienna Institute of BioTechnology, Universität für Bodenkultur Wien, Muthgasse 18, A-1190 Vienna, Austria, and the* [¶]*Institute for Organic Chemistry, Universität Wien, Währingerstrasse 38, A-1090 Vienna, Austria*

Background: Bacterial cell surface glycosylation impacts virulence.
Result: Surface layer glycans from *T. forsythia* are *O*-linked oligosaccharides that modify also multiple other *T. forsythia* proteins.
Conclusion: A general protein *O*-glycosylation system is present in *T. forsythia* sharing identical sequon requirements as other *Bacteroides* species.
Significance: Systematic protein *O*-glycosylation may affect the biology of *T. forsythia.*

Cell surface glycosylation is an important element in defining the life of pathogenic bacteria. *Tannerella forsythia* is a Gram-negative, anaerobic periodontal pathogen inhabiting the subgingival plaque biofilms. It is completely covered by a two-dimensional crystalline surface layer (S-layer) composed of two glycoproteins. Although the S-layer has previously been shown to delay the bacterium's recognition by the innate immune system, we characterize here the S-layer protein *O*-glycosylation as a potential virulence factor. The *T. forsythia* S-layer glycan was elucidated by a combination of electrospray ionization-tandem mass spectrometry and nuclear magnetic resonance spectroscopy as an oligosaccharide with the structure 4-Me-β-Man*p*NAcCONH$_2$-(1→3)-[Pse5Am7Gc-(2→4)-]-β-Man*p*NAcA-(1→4)-[4-Me-α-Gal*p*-(1→2)-]-α-Fuc*p*-(1→4)-[-α-Xyl*p*-(1→3)-]-β-Glc*p*A-(1→3)-[-β-Dig*p*-(1→2)-]-α-Gal*p*, which is *O*-glycosidically linked to distinct serine and threonine residues within the three-amino acid motif (D)(S/T)(A/I/L/M/T/V) on either S-layer protein. This S-layer glycan obviously impacts the life style of *T. forsythia* because increased biofilm formation of an UDP-*N*-acetylmannosaminuronic acid dehydrogenase mutant can be correlated with the presence of truncated S-layer glycans. We found that several other proteins of *T. forsythia* are modified with that specific oligosaccharide. Proteomics identified two of them as being among previously classified antigenic outer membrane proteins that are up-regulated under biofilm conditions, in addition to two predicted antigenic lipoproteins. Theoretical analysis of the S-layer *O*-glycosylation of *T. forsythia* indicates the involvement of a 6.8-kb gene locus that is conserved among different bacteria from the *Bacteroidetes* phylum. Together, these findings reveal the presence of a protein *O*-glycosylation system in *T. forsythia* that is essential for creating a rich glycoproteome pinpointing a possible relevance for the virulence of this bacterium.

In recent years, bacterial glycosylation systems have come under enhanced scrutiny because of the increasing frequencies with which they are seen in pathogenic and symbiont bacteria as well as their potential for exploitation in recombinant glycosylation engineering (1). Interestingly, in several of the investigated bacteria, a scenario of general glycosylation systems and of overlapping roles for distinct carbohydrate-active enzymes is evolving. For instance, the gastrointestinal pathogen *Campylobacter jejuni* targets multiple proteins at asparagine residues (2); the intestinal symbiont *Bacteroides fragilis* (3) and *Neisseria* species (1) possess general *O*-glycosylation systems; and in *Pseudomonas aeruginosa*, distinct stages of LPS, exopolysaccharide, and pilin glycoprotein biosynthesis share common enzymes (4, 5).

It is evident that cell surface-associated glycosylation, representing the contact zone of a bacterium with its immediate environment, is ideally suited to contribute to the bacterial physiology and to the bacterium-host cross-talk. In this context, we are investigating in this study the cell surface layer (S-layer)[3] protein glycosylation of the periodontal pathogen *Tannerella forsythia*. *T. forsythia* is a Gram-negative oral anaerobe that, together with the well studied *Porphyromonas gingivalis* and the spirochaete *Treponema denticola*, is a member of the "red complex" of microorganisms that inhabits the subgingival plaque biofilm (6) and is considered a major contributor to periodontal disease in humans (7). There are also reports on the

* This work was supported by the Austrian Science Fund projects P20605-B20 and P21954-B20 (to C. S.) and P20745-B11 (to P. M.).
[S] The on-line version of this article (available at http://www.jbc.org) contains supplemental Table S1 and Figs. S1 and S2.
[1] Both authors contributed equally to this work.
[2] To whom correspondence should be addressed. Tel.: 43-1-47654-2203; Fax: 43-1-4789112; E-mail: christina.schaeffer@boku.ac.at.

[3] The abbreviations used are: S-layer, surface layer; CID, collision-induced dissociation; Dig, digitoxose; ESI, electrospray ionization; KDO, 2-keto-3-deoxyoctulosonic acid; ManNAcA, *N*-acetylmannosaminuronic acid; ManNAcCONH$_2$, *N*-acetylmannosaminuronamide, PGC, porous graphitized carbon; Pse, pseudaminic acid; Pse5Am7Gc, 5-acetimidol-7-*N*-glycolyl-pseudaminic acid; ROESY, rotating frame Overhauser effect NMR spectroscopy; TOCSY, total correlated NMR spectroscopy; DMB, 1,2-diamino-4,5-methylene dioxybenzene dihydrochloride.

association of periodontitis with systemic diseases, such as cardiovascular diseases and diabetes (8, 9). Thus, there is great medical interest in understanding the bacterium-host cross-talk that forms the basis of health, disease, and healing.

Although a complete genome sequence is available for *T. forsythia* (available on the Oralgen Web site) relatively little is known about the virulence-associated factors of this bacterium (10). Because adhesion to oral surfaces constitutes the initial step in the bacterial colonization, identification of *T. forsythia* surface antigens that may play roles in these events is of primary interest. Sharma *et al.* (11) have identified a leucine-rich repeat BspA surface antigen that binds to fibronectin and other extracellular matrix components, whereas the *T. forsythia* S-layer was shown to mediate adhesion/invasion to human gingival epithelial cells and to epidermal carcinoma cells of the mouth (12, 13). Data on the virulence potential of the *T. forsythia* S-layer were supported in our laboratory by investigating the immune responses of human macrophages and gingival fibroblasts upon stimulation with wild-type (WT) *T. forsythia* and an S-layer-deficient mutant. This mutant induced significantly higher levels of the proinflammatory mediators IL-1β, TNF-α, and IL-8 compared with WT cells, especially at the early phase of response. This suggests that the S-layer attenuates the host immune response to this pathogen by evading its recognition by the innate immune system (14).

S-layers are water-insoluble proteins endowed with an intrinsic capability to self-assemble into a two-dimensional crystalline array that completely covers the bacterial cell surface, thereby obviously providing a selection advantage to the bacterium (15). Comparing *T. forsythia* with other S-layer-carrying bacteria, its status is unique. It is so far the only known Gram-negative bacterium that is covered with a glycosylated S-layer (16, 17), with, again uniquely, two S-layer glycoproteins being simultaneously present. The S-layer proteins TfsA (TF2661-TF2662; calculated molecular mass, 135 kDa) and TfsB (TF2663; calculated molecular mass, 152 kDa), that are encoded by an operon (18), share 24% amino acid similarity. They do not show overall homology to any other S-layer protein sequence deposited in databases, except for their C-terminal regions, which have profound similarity to putative S-layer glycoproteins of the phylogenetically closely related bacterium *Parabacteroides distasonis* (19). Although the glycosylation of the TfsA and TfsB proteins was already inferred some years ago from a positive carbohydrate staining reaction of an SDS-polyacrylamide gel (18), no details of the glycosylation aspect of the S-layer have been addressed so far. It is interesting to note that Honma *et al.* (6) have speculated about a link between cell surface glycosylation of *T. forsythia* and the biofilm life style of this bacterium, because with a *T. forsythia* mutant, possessing an insertional inactivation in the *wecC* (UDP-*N*-acetylmannosaminuronic acid dehydrogenase) gene (TF2055), coding for a predicted UDP-*N*-acetylmannosaminuronic acid dehydrogenase contained in a putative exopolysaccharide operon, increased cell surface hydrophobicity and, concomitantly, increased biofilm formation was observed (6).

To assess the significance of the S-layer glycosylation in *T. forsythia*, we deal in this study with the (i) elucidation of the S-layer glycan structure, (ii) determination of the glycosylation sites on the two S-layer proteins TfsA and TfsB, (iii) analysis of S-layer glycosylation in the *T. forsythia wecC* mutant with increased biofilm-formation, (iv) determination of the scope of the S-layer protein glycosylation system in *T. forsythia*, and (v) initial theoretical analysis of the genetic information underlying the glycosylation event.

EXPERIMENTAL PROCEDURES

Bacterial Strains, Medium, and Culture Conditions—*T. forsythia* wild-type strain ATCC 43037 (American Type Culture Collection) and defined mutants thereof were grown anaerobically for 4–7 days in enriched tryptic soy broth as described previously (14). The S-layer gene mutants *T. forsythia* Δ*tfsA* and Δ*tfsB*, respectively (13), were kindly provided by Yukitaka Murakami (Aichi-Gakuin University, Nagoya, Japan), and the *T. forsythia wecC* mutant (6) was obtained from Ashu Sharma (State University of New York at Buffalo). Cells were harvested by centrifugation (5,000 × *g*, 20 min, 4 °C), washed with 10 mM HEPES (pH 7.2), and stored at −20 °C until further processing.

SDS-PAGE and Blotting—SDS-PAGE was carried out on 7.5 or 8% slab gels in a Mini Protean electrophoresis apparatus (Bio-Rad) according to Laemmli (20). Proteins were visualized with colloidal Coomassie Brilliant Blue R-250 staining reagent, carbohydrates were visualized with Pro-Q Emerald 300 fluorescent stain (Invitrogen) (21), and the gels were imaged at 700 nm using the Odyssey imaging system (LI-COR) and at 300 nm using the Infinity-3000 (Vilber-Lourmat) apparatus, respectively. Tank blotting of (glyco)proteins to a polyvinylidene difluoride membrane was performed as described previously (22). Fucosylated structures on the proteins were detected by probing the blot with biotinylated *Aleuria aurantia* lectin (Szabo Scandic) at a concentration of 2 μg/ml. Detection was performed at 800 nm using streptavidin-conjugated IRDye® (LI-COR).

Isolation and Purification of the S-layer—For S-layer extraction, *T. forsythia* Δ*tfsB* and Δ*wecC* cells, respectively, were resuspended in 50 mM HEPES (pH 2.0) for 8 min/25 °C at a ratio of 1:3 (w/v), followed by neutralizing the suspension with 4 M NaOH and centrifugation (25,000 × *g*, 10 min, 4 °C); the extraction was repeated at least five times. The pooled supernatants were concentrated using Amicon Ultra-15 centrifugal filter units (50-kDa cut-off; Millipore), and the buffer was exchanged against 6 M urea in 30 mM ethanolamine (pH 10.4, buffer A) for subsequent anion exchange chromatography on a HighPrep 16/10 DEAE FF column (GE Healthcare). Bound proteins were eluted within 10 column volumes of a linear gradient of 0–100% 1 M NaCl in buffer A. Fractions were analyzed by SDS-PAGE, and the S-layer pool was subjected to size exclusion chromatography on Superdex 200 (XK26 column) with 6 M urea in 20 mM Tris/HCl (pH 7.2) as eluent. The S-layer pool was dialyzed against distilled H_2O and lyophilized. The protein content of the pool was determined using the Bio-Rad Bradford reagent.

Preparation of S-layer Glycopeptides—S-Layer glycopeptides for MS and NMR analyses were obtained upon proteolytic digestion of isolated S-layer protein of *T. forsythia* Δ*tfsB* and Δ*wecC*, 100 mg each, with Pronase E (Sigma) at 37 °C for 24 or 48 h, respectively (23). The degradation products were prepu-

rified using 250 mg of Superclean Envi-Carb cartridges (Sigma) followed by porous graphitized carbon (PGC)-HPLC for isolation and fractionation of glycopeptides, employing a Hypercarb column (100 × 3 mm; Thermo Fisher Scientific) with a gradient of 0–60% of 95% acetonitrile in ammonium formate buffer (0.3% formic acid, pH 3.0; flow rate, 0.6 ml/min).

S-layer O-Glycan Preparation—*O*-Glycans for MS and NMR analyses were released from purified TfsA S-layer protein by reductive β-elimination with 1 M $NaBH_4$ in 0.5 M NaOH at 50 °C overnight (24, 25). Excess salt was removed using a 25-mg HyperSep Hypercarb SPE cartridge (Thermo Fisher Scientific) according to published protocols (26–28). For purification of reduced *O*-glycans, preparative PGC-HPLC was performed as described above.

Furthermore, the TfsA and TfsB S-layer glycoproteins as well as four additional carbohydrate-positive protein bands were excised from SDS-polyacrylamide gels, and the *O*-glycans were isolated by applying in-gel reductive β-elimination. Briefly, excised gel slices were transferred to a plastic reaction tube, completely covered with 1 M $NaBH_4$ in 0.5 M NaOH, and incubated at 50 °C overnight, followed by removal of excess salt as described above. Borohydride-reduced glycans were subsequently analyzed by LC-ESI-MS/MS.

Ammonia-based non-reductive β-elimination was done according to a protocol of Huang *et al.* (29), with slight modifications. Briefly, glycan-positive protein bands were covered with ammonium hydroxide solution (25%), which was saturated with ammonium carbonate. Further, 100 mg of ammonium carbonate were added to the reaction tube, and the mixture was incubated at 60 °C for 24 h. After desalting, the reaction product was analyzed by LC-ESI-MS/MS.

Monosaccharide Analysis—Monosaccharide analysis of the borohydride-reduced S-layer *O*-glycans was performed on a purified fraction after PGC-HPLC. The glycans were hydrolyzed with 25% TFA for 1 h at 100 °C, and released monosaccharides were analyzed as anthranilic acid derivatives by HPLC (30). Fluorescence detection was performed at 360-nm excitation and 425-nm emission, respectively. To identify the reducing end sugar, labeling was done immediately after non-reductive glycan release (31) and before hydrolysis with TFA.

Labeling with 1,2-diamino-4,5-methylene dioxybenzene dihydrochloride (DMB) and purification of the pseudaminic acid (Pse) derivative for MS and NMR analysis were performed after incubation of a purified *O*-glycan fraction or, in the case of a large scale preparation, of whole *T. forsythia* WT cells with 1 M TFA (1 h, 80 °C). Subsequently, cells were centrifuged (15,000 × *g*, 10 min), and the supernatant was collected and lyophilized. The lyophilisate was subsequently dissolved in a 1:1 (v/v) mixture of solution A (1 mg of DMB in 0.317 ml of MilliQ water) and solution B (1 mg of $Na_2S_2O_4$, 47 μl of acetic acid, 41 μl of 2-mercaptoethanol in 0.205 ml of MilliQ water) and incubated for 2 h at 56 °C. Insoluble particles were removed by centrifugation (20,000 × *g*, 5 min), and the supernatant was applied to reverse phase HPLC (Hypersil ODS, 250 × 4 mm). Buffer A consisted of 50 mM ammonium acetate (pH 5.5), and a gradient was performed from 11 to 14% buffer B (95% acetonitrile) within 8 min on a Shimadzu HPLC system consisting of a LC-10AD pump system, a RF-10AXL detector, and a SCL-10Avp controller. Fluorescence detection was done at 373-nm excitation and 448-nm emission (32).

LC-ESI-MS/MS—Borohydride-reduced *O*-glycans were analyzed by PGC-ESI-MS/MS as described recently (Hypercarb, 0.32 × 150 mm, inner diameter 5 μm) (28, 33). Ammonium formate buffer (0.3% formic acid, pH 3.0) was used as buffer A, and a gradient was performed from 0 to 35% acetonitrile within 35 min using a Dionex Ultimate 3000 (cap flow, 8 μl/min). Detection was done by an ESI-Q-TOF Global Ultima from Micromass (Waters). Data were evaluated using MassLynx 4.0 software. MS/MS experiments were performed at 30% collision energy using CID with argon gas.

High Resolution Mass Spectrometry and Accurate Mass Measurements—High resolution MS and accurate mass measurements were performed on a LTQ Orbitrap-Velos (Thermo Fisher Scientific) at the Thermo Fisher Scientific demonstration center. HPLC-fractionated, borohydride-reduced S-layer *O*-glycans were analyzed by direct infusion on a nanospray emitter in MS and MS/MS mode.

Proteomics—To identify protein portions of presumptive *T. forsythia* glycoproteins, an in-gel trypsin digest of the respective bands on SDS-polyacrylamide gels was performed. Extracted proteolytic peptides were further subjected to reverse phase liquid chromatography coupled to ESI-MS/MS (28, 34). The X!tandem algorithm (see the Global Proteome Machine Web site) was used for a protein database search of tandem MS data obtained from tryptic peptides. Results were further evaluated using log(*e*) values to estimate correctness of peptide assignments.

NMR Spectroscopy—The isolated *O*-glycans and sugar derivatives were lyophilized and dissolved in D_2O (99.99% D; Sigma-Aldrich) to concentrations of ~500 μg/600 μl. The solutions were transferred into 5-mm NMR sample tubes (Promochem). Spectra were recorded on a Bruker DRX-600 AVANCE spectrometer (Bruker) at 600.13 MHz (^1H) using the Bruker Topspin 1.3 software. One-dimensional proton spectra were measured with presaturation during a 1.0-s relaxation delay and acquisition of 32,000 data points. Zero filling to 64,000 data points and Fourier transformation led to spectra with a 7,200-Hz range. Two-dimensional COSY, TOCSY (100 ms mixing time), and ROESY (400-ms mixing time, *O*-glycans) or NOESY (800-ms mixing time, sugar derivates) spectra were measured using standard Bruker programs. Therefore, 384 experiments with 2,048 data points and an appropriate number of scans were recorded, each. After linear forward prediction to 512 data points in the f_2 dimension and sinusoidal multiplication in both dimensions, they were Fourier transformed to two-dimensional spectra with a 6,000 Hz range in both dimensions. The diffusion behavior of the monosaccharide was derived from the signal attenuation in a series of stimulated echo spectra with increasing gradient amplitudes by fixed diffusion delay (35, 36). All measurements were performed at 298.1 K. Chemical shifts were referenced to external acetone (δ_H 2.225 ppm).

Genome Sequence Analysis—A 6.8-kb gene locus comprising ORFs TF2049–TF2055, including the previously described exopolysaccharide operon (TF2053–TF2055) (6), which is predicted to be involved in protein glycosylation, was analyzed and screened for homologous sequences in the phylogenetically

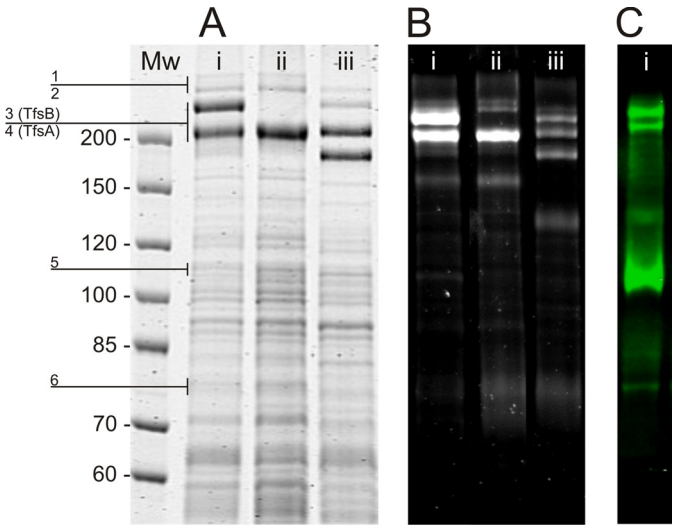

FIGURE 1. *A*, Coomassie Brilliant Blue R-250-stained SDS-PAGE gel (7.5%) of crude cell extracts from *T. forsythia* WT and mutants used in this study. *Mw*, PageRuler unstained protein ladder (Fermentas); *lane i*, *T. forsythia* WT; *lane ii*, *T. forsythia* Δ*tfsB*; *lane iii*, *T. forsythia* Δ*wecC*. The S-layer glycoprotein bands TfsA and TfsB (identity confirmed by proteomic analyses; data not shown) as well as *bands 1* and *2* are significantly downshifted in *T. forsythia* Δ*wecC* cells as a result of truncated S-layer glycosylation. *B*, Pro-Q Emerald carbohydrate-stained gel (8%). *C*, blot of a *T. forsythia* WT whole cell extract after separation by SDS-PAGE (8% gel) probed with *A. aurantia* lectin. Prominent bands (*1–6*) giving a positive signal in both Coomassie Brilliant Blue R-250 and carbohydrate-stained gels were excised and subjected to glycoproteomics analysis (see Table 2).

related organisms *B. fragilis* NCTC 9343, *Bacteroides thetaiotaomicron* VPI 5492, *Bacteroides uniformis* ATCC 8492, *P. gingivalis* ATCC 33277, and *Parabacteroides distasonis* ATCC 8503 using the comparative genomics platform CoGe (available on the World Wide Web). The highest scoring sequences (*E* value $<10^{-5}$) were extracted and analyzed for comparable cluster formation within the respective genomes.

RESULTS

General Description of the S-layer Proteins TfsA and TfsB—*T. forsythia* possesses two S-layer glycoproteins that are abundant in a whole cell lysate of the bacterium and exhibit apparent molecular masses of ~230 and 270 kDa, respectively, on an SDS-polyacrylamide gel (Fig. 1*A*). This is indicative of a modification of the ~135- and ~152-kDa S-layer proteins by glycosylation as confirmed by a strong staining reaction with the Pro-Q Emerald reagent (Fig. 1*B*). Interestingly, both S-layer proteins are downshifted in *T. forsythia* Δ*wecC*, which could later be correlated with the presence of truncated S-layer glycans (Fig. 1, *A* and *B*, *lanes iii*).

*Glycan Profile of O-Glycans from the S-layer Proteins TfsA, TfsB, and TfsB*Δ*wecC*—In-gel reductive β-elimination was employed to release glycans from the protein backbone. Mass analysis was followed by PGC-ESI-MS/MS. For the TfsA and TfsB proteins, three dominant glycan structures were observed with monoisotopic values of 1,621, 1,751, and 1,897 Da (Fig. 2). CID fragmentation analysis of the 1,621-Da glycan unit revealed it to be a hetero-oligomer consisting of eight different sugar residues (Fig. 3). Mass increments for one pentose, one deoxyhexose, three uronic acids (modified or free), one methylhexose, and one reduced hexose in addition to one so far unknown glycose residue were identified. To some extent, the oligosaccharides were substituted by one dideoxyhexose and, further, with one more deoxyhexose, leading to the above described mass pattern. Additionally, the ESI-MS spectrum showed a minor peak with a mass difference corresponding to a methylhexose (Fig. 2). Interestingly, glycans analyzed from both TfsA and TfsB S-layer proteins showed identical glycan mass profiles, indicating the presence of one uniform glycosylation pattern. The TfsB protein derived from the Δ*wecC* mutant showed a similar glycan pattern but was devoid of two *N*-acteylhexosaminuronic acid residues and the yet non-described 361-Da sugar (Fig. 2).

Monosaccharide Composition Analysis—To investigate the nature of the monosaccharide constituents of the *T. forsythia* S-layer *O*-glycans, the isolated and HPLC-purified 1,621-Da *O*-glycan was hydrolyzed with 4 M TFA to its monosaccharide components and analyzed as anthranilic acid derivates using reverse phase chromatography. The HPLC profile compared with standard sugars clearly identified the presence of a fucose and a xylose residue. By using non-reductive β-elimination for *O*-glycan release and anthranilic acid labeling, galactose was identified as reducing sugar, linking the S-layer glycan to the protein backbone (data not shown).

High resolution MS/MS measurements (LTQ Orbitrap-Velos instrument) of the intact and borohydride-reduced *O*-glycan further allowed the determination of the sum formula for each of the constituting monosaccharides. By this method, the presence of one pentose, one deoxyhexose, one dideoxyhexose, one methylated hexose, one hexuronic acid, one *N*-acetylated hexuronic acid, and one *N*-acetyl-*O*-methylhexuronic acid was confirmed (supplemental Table S1).

The structures of all sugar residues were further specified by NMR spectroscopy. Here, we identified the methyl-hexose as methyl-galactose and the two *N*-acteylhexosaminuronic acid residues as *N*-acetylmannosaminuronic acid and as *O*-methyl-*N*-acetylmannosaminuronic acid, respectively. The dideoxyhexose that was already observed in the MS/MS fragmentation profile was identified as a digitoxose.

One final sugar residue remained unclear, even after high resolution MS/MS and NMR analysis of the intact *O*-glycan. No structure of a known sugar fitted to its exact mass and calculated sum formula ($C_{14}H_{25}O_9N_3$) as determined by high resolution MS. To unravel this unusual component, a nucleotide sugar screening was performed to identify the pool of activated sugars in the bacterial cytosol (supplemental Fig. S1). A plethora of well known sugar precursors, including GDP-Fuc, UDP-Glc, UDP-Gal, TDP-Rha, UDP-HexNAcs, and UDP-GlcA, were detected (37) in addition to an at first inexplicable peak mass at 683.2 Da $(M-H)^-$. CID fragmentation revealed it to be a CMP-activated sugar with exactly the mass found for the yet unidentified *O*-glycan constituent. Remarkably, this CMP-activated sugar was present in high concentration exceeding that of house-keeping nucleotide sugars, such as UDP-Glc. Because mainly α-keto sugars are known to be activated by CMP (*e.g.* CMP-*N*-acetylneuraminic acid, CMP-KDO, CMP-Pse), this was a first hint of the identity of the unknown compound. Further similarities in the fragmentation pattern to those of sialic acids strongly indicated the presence of an α-keto

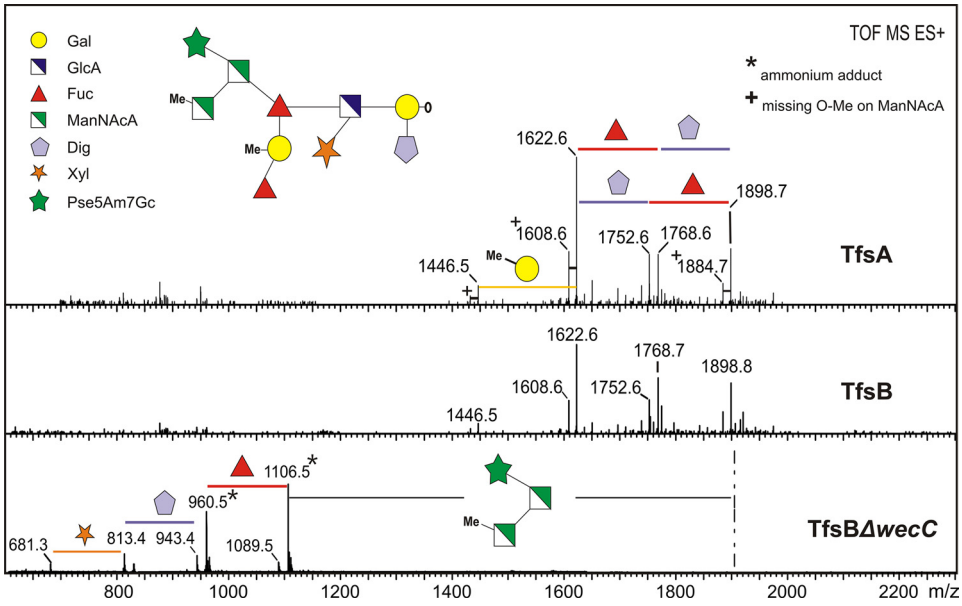

FIGURE 2. **Deconvoluted ESI-TOF-MS spectrum of TfsA, TfsB, and TfsBΔ*wecC* *O*-glycans.** Three main structures were observed after reductive β-elimination, representing variations in Fuc and Dig residues. The terminal *O*-Me-ManNAcA residue was found to be generated from its amide derivate during β-elimination (see "Results"). Minor amounts of each structure missing the *O*-methylation on this mannosaminuronamide residue were also detected. TfsB *O*-glycans from the *wecC* mutant lack the three-sugar branch, consisting of ManNAcA, $ManNAcCONH_2$, and the Pse derivate.

acid. DMB labeling of a hydrolysate of the *O*-glycan followed by reverse phase HPLC analysis led to a large peak in the elution region of sialic acids. The mass of the DMB-labeled sugar fitted to the unknown sugar residue. Despite its mass differing from that of DMB-labeled *N*-acetylneuraminic acid, the unknown derivative had a similar retention behavior and also a very similar fragmentation pattern in ESI-MS/MS.

Combined NMR analyses of the purified DMB-labeled sugar residue and of the complete oligosaccharide revealed the presence of a non-2-ulosonic acid carrying two substituents on the amino functions in position C5 and C7. A free methyl group in position 9 was identified by its characteristic ^{1}H NMR shift. Position C5 carries an acetimidol group (Am) showing a weak NOE between the CH_3 group and the H in position 5. In position 7, an *N*-glycolyl group (Gc) is bound, which could also be identified and localized by typical ^{1}H NMR shifts and weak NOEs. This substitution pattern of the DMB-labeled sugar is in agreement with the respective ESI-MS/MS results. Further signals present in the ^{1}H NMR spectra of the DMB-labeled sugar residue were studied by diffusion measurements and were identified to belong to an impurity (35, 36). Comparison of all recorded NMR spectroscopic data of the *O*-glycan with those of the isolated $C_{14}H_{25}O_9N_3$ unit showed good concordance. The configuration of the non-2-ulosonic acid has been proven by the few detectable $^3J_{H\text{-}H}$ couplings and NOEs and is in better accordance with those of a pseudaminic acid residue than with those of legionaminic acid. The whole $C_{14}H_{25}O_9N_3$ unit can hence be considered as Pse5Am7Gc.

Presence of a Mannosaminuronamide, Which Is Hydrolyzed during β-Elimination to Mannosaminuronic Acid—Upon fragmentation of potential glycopeptides during glycosylation site analysis of the *T. forsythia* S-layer proteins, a mass difference of 1 Da between released and bound *O*-glycan was encountered. After comparison of MS/MS data, the mass difference was found to be present at the *O*-Me-ManNAcA residue, which was 1 Da larger after reductive β-elimination. Further experiments showed that the strong base treatment led to this mass change and gave a first indication of its nature. As already shown in a previous study (38), mannosaminuronic acids can be found as amide derivates in bacteria. To verify this, a non-reductive β-elimination was performed using ammonia carbonate (29). Although the previously observed mass shift could not be detected in that case, further exposure to sodium hydroxide for several h at 50 °C led to a deamidation reaction. Further exact mass measurement of ammonia carbonate-released glycans proved our assumption of amide hydrolysis due to strong base exposure (data not shown).

NMR Spectroscopy of O-Glycans—Knowing the structure of all nine saccharide units, the interglycosidic connections could be determined. For the determination of such structural details, only ^{1}H NMR (Fig. 4, *A* and *B*) and homonuclear two-dimensional NMR spectra were applicable, because the small amounts of purified *O*-glycans did not allow us to record ^{13}C resonances with adequate signal/noise ratio. Based on mass spectrometric and wet chemical analyses, however, COSY and TOCSY spectra enabled the identification of the monosaccharide units. ^{1}H chemical shifts and coupling constants allowed the analysis of anomeric configurations. ROESY spectra provided further information about spatial closeness of anomeric protons, which enabled the determination of the interglycosidic linkages.

The S-layer oligosaccharide isolated from *T. forsythia* WT cells consists of nine monosaccharide units, which form a branched system (Fig. 4*C*). This system, however, formed two conformers. They were distinguishable in NMR spectra (and liquid chromatography) and, hence, led to two sets of signals in a ~3:1 ratio, which showed exchange spectroscopy cross-peaks in ROESY spectra. Consequently, not all chemical ^{1}H shifts

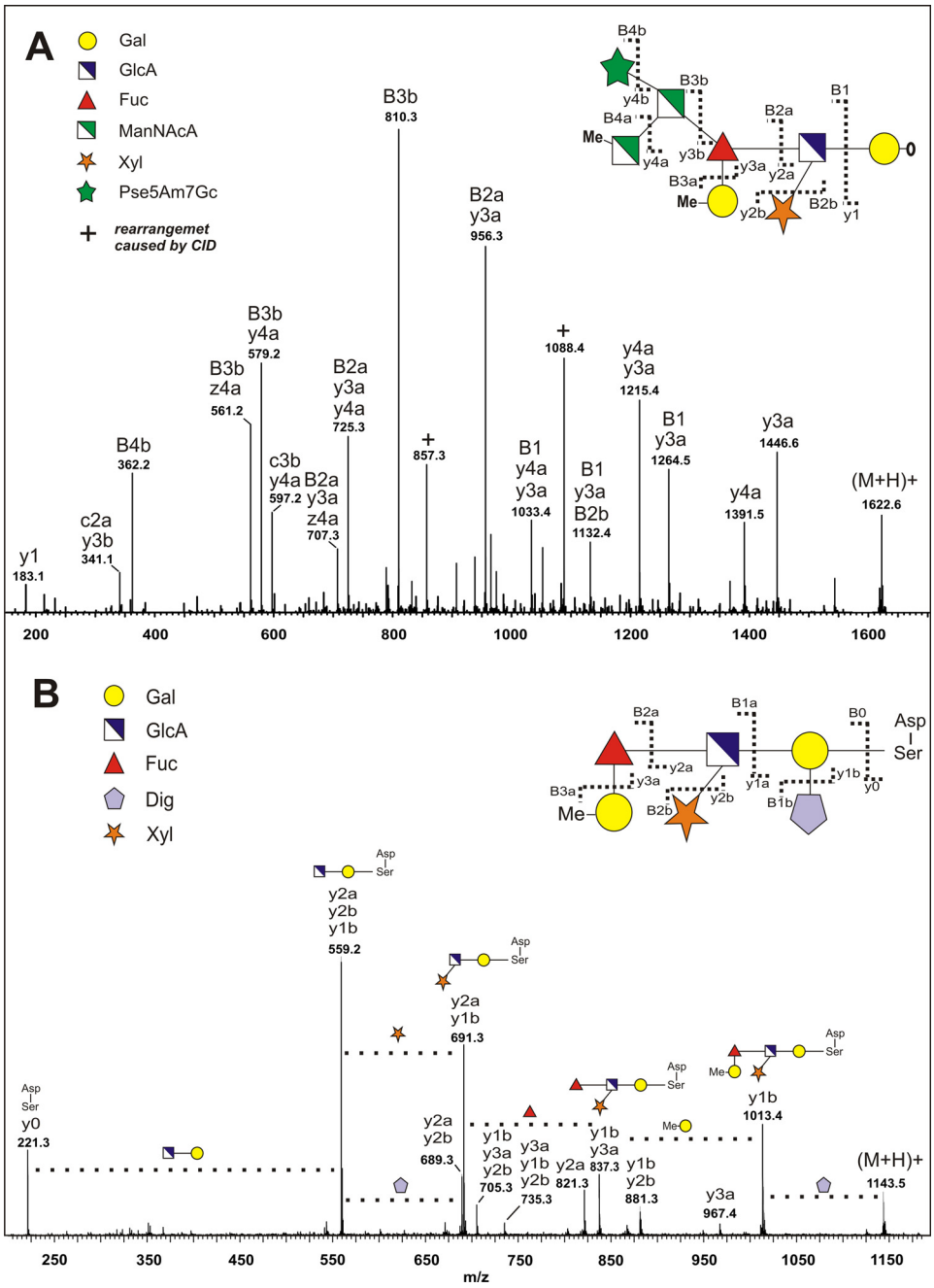

FIGURE 3. *A*, ESI-TOF-MS/MS spectrum of the borohydride-reduced *O*-glycans, as observed for all identified glycoproteins in *T. forsythia*. Protonated ions showed rearrangement artifacts of the Xyl residue during CID, which could be avoided by fragmentation of sodium adducts (53). Gal was found as reducing sugar (reduced by borohydride, gain of 2 Da), followed by a GlcA, Fuc, and *O*-Me-Gal. A branch, consisting of two mannosaminuronic acids (one was found to be a mannosaminuronamide before base treatment during β-elimination) and Pse5Am7Gc, is linked via the Fuc residue to the glycan core. During fragmentation, this chain gave a characteristic fragment peak series (B3b, B3b/Y4a, B4b) which was observed in all acquired MS/MS spectra. Note that fragment ions labeled with more than one ion series annotation are derived from multiple cleavage events. *B*, ESI-TOF-MS/MS spectrum of glycopeptides obtained from a Pronase digest of *T. forsythia* Δ*wecC*, on which a truncated *O*-glycan lacking the ManNAcCONH$_2$-Pse5Am7Gc branch was found. In this case, the α1*O* glycosidic linkage of Gal was found to serine, which is always preceded by an aspartic acid residue.

could be determined, but all data of the indicative positions were identified.

The carbohydrate unit linked to the protein was identified from a non-reduced sample preparation as an α-Gal*p* (**1**). This galactose unit carries a terminal β-Dig*p* (**2′**) (39) linked to its position 2 and a 1→3-bound β-Glc*p*A (**2**). The latter one is part of the oligosaccharide backbone and carries an α-Xyl*p* branch (**3′**) linked to its position 3. The next unit in the backbone has been identified as an α-Fuc*p* (**3**), which is 1→4-linked to the β-Glc*p*A (**2**). This fucose carries a 1→2-linked α-Gal*p* (**4′**), which is methylated on its position 4. A β-Man*p*NAcA (4, 40), the next unit in the backbone, is 1→4-bound to the fucose residue (**3**). It carries on its position 3 a β-Man*p*NAc-CONH$_2$ (5, 40), which is methylated on position 4 and represents the terminal unit of the backbone. Additionally, the above described Pse5Am7Gc (**5′**) is bound to the Man*p*-

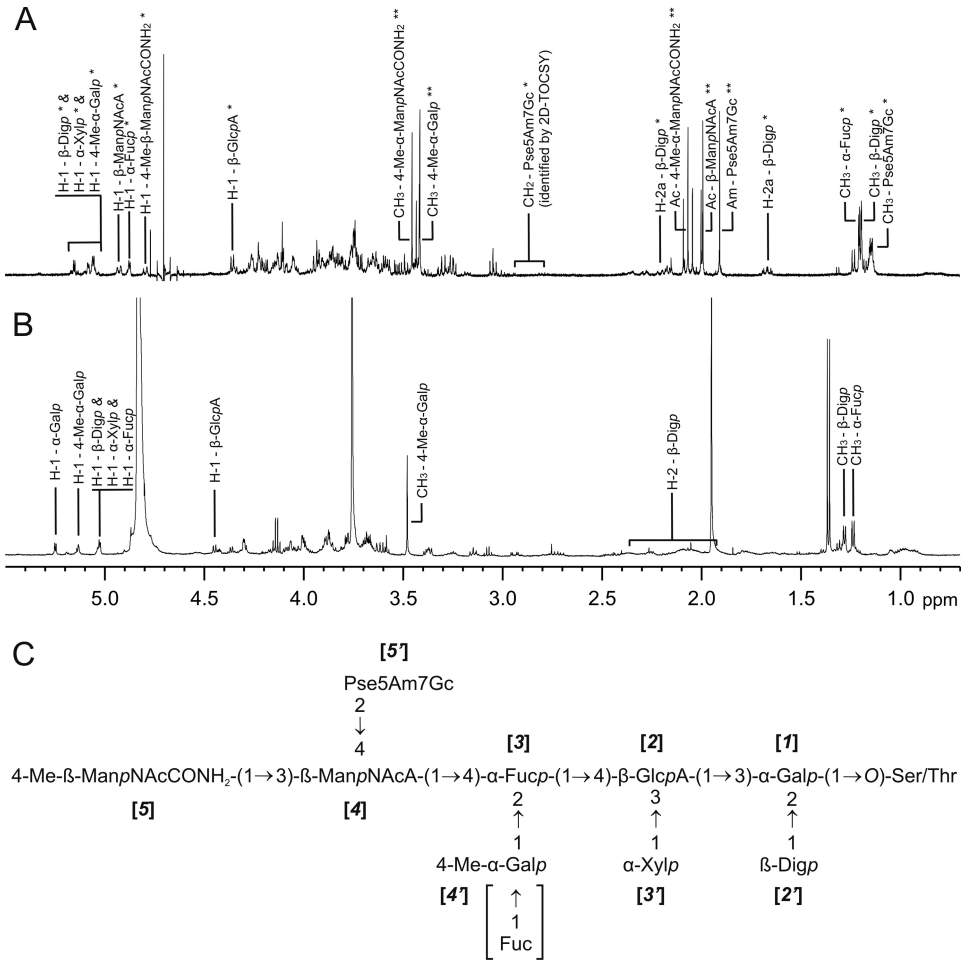

FIGURE 4. *A*, 600-MHz ^{1}H NMR spectrum of the S-layer oligosaccharide from *T. forsythia*. *B*, 600-MHz ^{1}H NMR spectrum of a glycopeptide from the Δ*wecC* strain (see also Fig. 3*B*). Both spectra were recorded in D_2O at 297 K. Signals of indicative protons are marked with their assignment. In *A*, overlapping groups of signals from both isomers are marked with *one asterisk*, whereas in the case of separable singles only the signals of the major isomer are indicated with *double asterisks*. *C*, structure of the S-layer oligosaccharide of *T. forsythia* as determined by combined MS and NMR analysis.

NAcA residue (**4**), quite likely in position 4, because this is the only possible position. The configuration of the anomeric center at position 2 in the Pse5Am7Gc (**5′**) was not determined. A further fucose was detected by MS to be bound to the galactose unit (**4′**). This fucose residue, however, is present in substoichiometric amounts and was not identified in the NMR spectra.

The oligosaccharide isolated from the *T. forsythia wecC* mutant consisted only of six glycose units. This smaller oligosaccharide did not show distinguishable signal sets of two conformers and, therefore, has a higher degree of freedom between different conformers. It was identified to be a partial structure of the above described S-layer oligosaccharide. In that structure, the Man*p*NAcA unit (**4**) and 4-Me-β-Man*p*NAcCONH$_2$ unit (**5**) as well as the PseAm7Gc (**5′**) were missing. The backbone, hence, consists of the 4-Me-α-Gal*p*-(1→2)-α-Fuc*p*-(1→4)-β-Glc*p*A-(1→3)-α-Gal*p*-(1, which is bound to the protein. The branching β-Dig*p* (**2′**) and the α-Xyl*p* (**3′**) are again 1→2-linked to α-Gal*p* (**1**) and 13-linked to β-Glc*p*A (**2**), respectively. Fig. 4*C* shows a representation of the larger oligosaccharide, and several indicative ^{1}H NMR spectroscopic shifts of both oligosaccharides are listed in Table 1. The complete S-layer oligosaccharide isolated from *T. forsythia* is an overall highly diverse structure composed of four oxidized sugars (one is present as hexuronamide), up to three deoxy residues and two *O*-methyl modifications.

General Glycosylation Profile of T. forsythia Glycoproteins—At a closer examination, the carbohydrate-stained SDS-polyacrylamide gel of *T. forsythia* whole cell lysates indicated, besides the S-layer glycoproteins, the presence of several other glycosylated proteins in the molecular mass range between 60 and 250 kDa (Fig. 1*B*). Some of those bands were also reactive with the fucose-specific *A. aurantia* lectin, which perfectly detects the S-layer glycans (Fig. 1*C*). Thus, it was conceivable to assume that the S-layer *O*-glycosylation system would affect also other *T. forsythia* proteins.

Four prominent bands (*Bands 1, 2, 5, 6* as indicated in Fig. 1*A*) were excised from the gel and subjected to in-gel reductive β-elimination as used for the S-layer glycoproteins. Surprisingly, all bands showed the same glycan profile as obtained for the S-layer glycoprotein bands, with slight variations detected in their relative ratios and in *O*-methylation of the mannosaminuronamide residue (Fig. 5). In negative controls performed with SDS-polyacrylamide gel pieces from gel slices without Coomassie Brilliant Blue R-250 staining, no glycans were detected.

TABLE 1

^{1}H NMR chemical shift data (ppm) of the S-layer oligosaccharide of TfsA (top) and of the S-layer glycopeptide from *T. forsythia* Δ*wecC* (bottom)

Listed are the shifts of the major conformer. ND, not determined.

Unit	H-1	H-2	H-3	H-4	H-5	H-6	H-7	H-8	H-9	Ac	Me
α-Gal*p* (**1**)[a]	ND	ND	ND	ND	ND	ND					
β-Glc*p*A (**2**)	4.46	3.37	3.70	3.62	4.16						
β-Dig*p* (**2′**)	5.09	2.18 and 1.68	3.85	3.06	3.64	1.21					
α-Fuc*p* (**3**)	4.89	3.84	3.88	4.01	4.36	1.24					
α-Xyl*p* (**3′**)	5.08	3.44	3.65	ND	ND						
β-Man*p*NAcA (**4**)	4.91	4.21	4.08	ND	ND					1.99	
4-Me-α-Gal*p* (**4′**)	5.06	3.71	3.44	4.13	ND	ND					3.43
4-Me-β-Man*p*NAcCONH$_2$ (**5**)	4.73	4.18	3.84	ND	ND					2.06	3.46
Pse5Am7Gc (**5′**)[b]			2.95 and 2.78	4.15	3.82	4.23	3.98	3.66	1.14	1.91	
Glycolyl (of **5′**)[b]		3.63 (2H)									
α-Gal*p* (**1**)	5.25	3.89	3.67	4.30	ND	ND					
β-Glc*p*A (**2**)	4.46	3.35	3.68	3.60	4.15						
β-Dig*p* (**2′**)	5.04	2.25 and 1.80	3.88	3.15	4.07	1.28					
α-Fuc*p* (**3**)	5.03	3.96	4.04	4.01	4.37	1.21					
α-Xyl*p* (**3′**)	5.05	3.51	ND	ND	ND						
4-Me-α-Gal*p* (**4′**)	5.14	3.67	3.86	4.27	ND	ND					3.48

[a] Identified from glycopeptide sample listed in the bottom.
[b] Identified from DMP-labeled sample of Pse5Am7Gc.

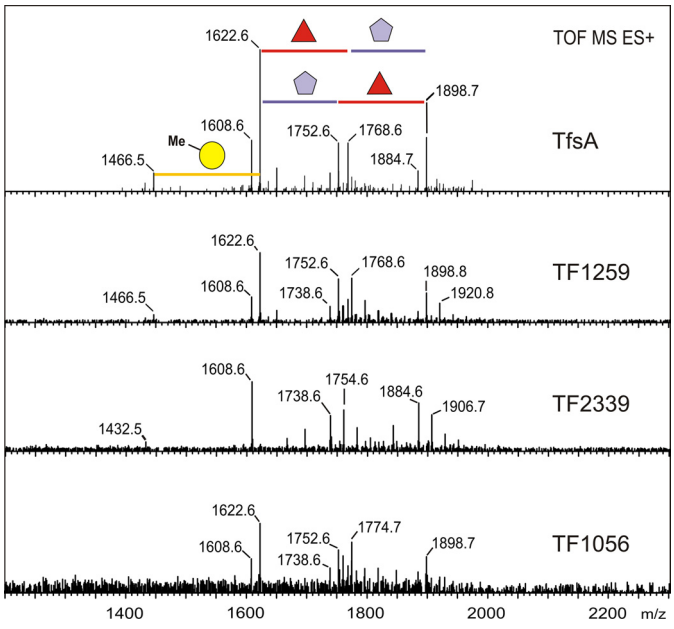

FIGURE 5. **Deconvoluted ESI-TOF-MS spectra of glycans released from *T. forsythia* glycoprotein bands after in-gel β-elimination in comparison with TfsA *O*-glycans.** Proteins were identified as TF1259 (*band 1* in Fig. 1*A*), TF2339 (*band 2*), and TF1056 (*band 5*) by a proteomics approach (compare with Table 2). *O*-Glycans were found from all proteins as identical and just varying in their relative ratios as well as in *O*-methylation of the mannosaminuronamide residue.

Glycan profiles were analyzed by PGC-ESI-MS/MS exactly as done for the S-layer *O*-glycans. Elution times of individual glycoforms and their MS/MS fragmentation patterns were identical for all analyzed bands.

Identification of O-Glycosylated Proteins and Determination of a General Glycosylation Motif—To identify the other proteins carrying the S-layer oligosaccharide, the bands indicated in Fig. 1*A* were excised from the SDS-polyacrylamide gel, proteolytically digested, and subjected to reverse phase ESI-MS/MS peptide mapping.

Using the Oralgen proteome data base (available on the World Wide Web), tryptic peptides could be assigned to individual ORFs, allowing the identification of further proteins; these were TF1259, TF2339, TF1056/TF1150, and TF0091. From two proteins (TF2339 and TF1259) glycopeptides were identified and, upon a Pronase digest (described below), glycosylation sites could be assigned. Due to the low abundance of TF0091 and TF1056, it was impossible to detect glycopeptides by applying that strategy. Notably, TF1150 was co-isolated with TF1056 but without a hint for glycosylation. So far, there are no discrete functions associated with the identified proteins.

Table 2 summarizes all identified proteins (including TfsA and TfsB) together with the detected glycosylation sites. Interestingly, all identified glycosylation sites match the D(S/T)(A/I/L/M/T/V) three-amino acid motif that was recently described for the general protein *O*-glycosylation system in *B. fragilis* (3).

To extend the glycosylation motif analysis to a broader range of proteins, a protein pool out of 1 g of *T. forsythia* cell extract was prepared, and a 24-h proteolytic digest using Pronase was generated to yield incomplete digestion. The pool of prepurified glycopeptides was subsequently analyzed by PGC-ESI-MS/MS. A series of small glycopeptides was identified (supplemental Fig. S2), matching the *O*-glycosylation motifs found in the work of Fletcher *et al.* (3).

O-Glycans Are Linked via Galactose to Serine/Threonine Residues—The Pronase digest of the S-layer protein extract from the *T. forsythia wecC* mutant was purified by PGC-HPLC and analyzed by NMR, which showed that galactose is 1*O*-linked to serine and threonine (data not shown). This is in agreement with the finding of galactose as the reducing sugar (see above).

Theoretical Analysis of Protein O-Glycosylation in T. forsythia—The gene locus Tf2055-Tf2049 contains a predicted WecC (TF2055), a predicted UDP-*N*-acetylglucosamine 2-epimerase (NeuC, TF2054), three predicted glycosyltransferases (TF2053, TF2050, and TF2049), a predicted acetyltransferase (TF2052), and one ORF with yet unassigned function (TF2051).

As shown in our study, deletion of TF2055 causes truncation of S-layer protein glycans by lacking the 809-Da Pse-containing trisaccharide side branch. This implicates that this genomic region unambiguously carries crucial information for proper surface glycan assembly. We compared the ORFs comprising that 6.8-kb locus with sequences from phylogenetically related

TABLE 2

Proteomic analysis of tryptically digested protein bands as indicated in Fig. 1*A*

Glycopeptides and their respective glycosylation sites were identified for bands 1–4. *O*-Glycosylation occurs at the three-amino acid motif D(S/T)(A/I/L/M/T/V) (underlined). Protein sequences and accession numbers were extracted from the Oral Pathogen Sequence Database. ND, not detected.

Band	Protein	Mass (observed/calculated)	Unique peptides	Glycopeptides	Glycosylation site
		kDa			
1	TF1259	>270/240	>5	NIITGDTVNFR	Thr^{1082}
2	TF2339	>270/200	>15	VPPADIVLGDTAINTVIK	Thr^{107}
				IHTDTASTSGFK	Thr^{593}
				YFVDTLR	Thr^{1433}
3	TfsB/TF2663	270/152	>25	FATDSVVR	Ser^{473}
				LMVDTLPR	Thr^{493}
				DTATVNLYAFNY	Thr^{752}
				DGTGRDSLIY	Thr^{786}
				TAIYVDTAYVNR	Thr^{1069}
4	TfsA/TF2661-2	230/135	>25	TCGASDSVR	Ser^{197}
				FNTTDESAIGSDNPDTLKFHR	Thr^{819}
				NQTDSAR	Ser^{943}
				LSFVPAIHAGDTLYILNGRPIEAFIQK	Thr^{979}
5	TF1056	110/72	>5	ND	ND
	TF1150	110/100			
6	TF0091	80/42	>5	ND	ND

species and found the said genes present in high homology and clustered within very short distances in the respective genomes (Fig. 6). Interestingly, in *B. fragilis*, homologues are highly clustered within a locus, which was proven to result in a glycosylation defect of surface proteins upon full knock-out (3). *T. forsythia* also encodes a flippase upstream of that predicted glycosylation locus (Tf2076), which is highly homologous to the annotated flippases found within the clusters of selected organisms. Although not in immediate proximity to the locus, this enzyme might be crucial for catalyzing the transport of the glycan moiety to the periplasmic space.

DISCUSSION

A reduction of oral pathogens and their virulence factors is a prerequisite for the maintenance of both general and oral health. Especially those factors that are associated with the bacterial cell envelope and/or exposed to the environment are prime candidates for mediating virulence through their direct involvement in pathogen-host interactions. In this context, cell surface carbohydrates of various pathogenic species as manifested in the forms of LPS, capsules, or glycoprotein glycans are of primary interest, taking also into account their well established status as ligands of innate and adaptive immune effectors.

In this study, a first approach was undertaken to characterize the cell surface glycosylation of *T. forsythia*, a bacterium that has emerged as a crucial periodontal pathogen (7). Considering that this bacterium can affect systemic health, *T. forsythia* and especially its mechanisms governing pathogenicity deserve detailed investigation.

This study in combination with detailed microscopic investigations in our laboratory[4] revealed that the cell surface architecture of *T. forsythia* is so far unique, with a typical Gram-negative cell envelope profile being overlaid with an ~22-nm-thick, closed, monolayer that is formed by co-assembly of the two *T. forsythia* S-layer glycoproteins. Whereas the TfsA and TsfB S-layer protein portions are antigenically diverse according to immunoblot evidence,[4] identical oligosaccharides are displayed at multiple sites on either S-layer protein via *O*-glycosidic linkage units between α-D-Gal*p* and Thr and Ser residues, respectively, that are scattered over the whole S-layer proteins. According to combined 600.13-MHz ^{1}H NMR/LC-ESI-MS approaches, the *T. forsythia* S-layer oligosaccharide is an overall highly diverse and branched structure containing several modified glycose residues (compare with Fig. 4*C*). This structure contradicts the so far valid building plan of bacterial S-layer glycans, which have been described as long-chain heteropolysaccharides composed of individual repeating units (17, 18), and, thus, is reminiscent of archaeal S-layer glycans (41). Although uncommon sugar residues, such as α-D-Fuc*p*NAc, β-D-Qui*p*NAc, or β-D-*glycero*-D-*manno*-Hep*p* are known to occur in bacterial S-layer glycans, this is the first report on an α-L-Fuc*p* residue (the L-configuration was inferred from the presence of GDP-Fuc (supplemental Fig. S1), which is the common nucleotide-activated form of L-Fuc), a digitoxose, a ManNAcA, a $ManNAcCONH_2$, and a modified pseudaminic acid (Pse5Am7Gc) in an S-layer glycan. It is tempting to speculate

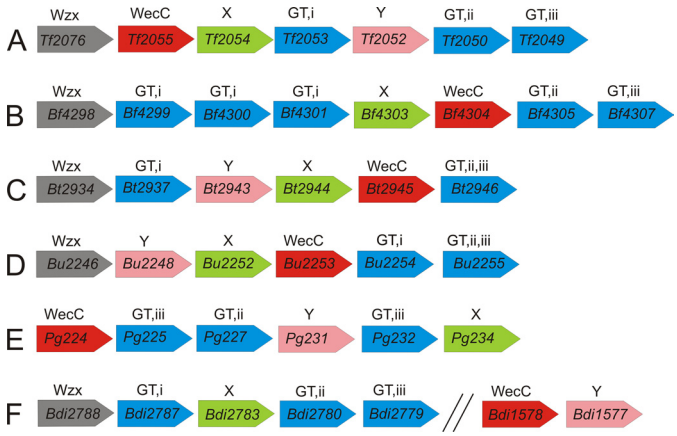

FIGURE 6. Predicted *O*-glycosylation gene locus in *T. forsythia* (*A*). Clustering of highly homologous genes was observed in different *Bacteriodetes* species, including *B. fragilis* NCTC 9343 (*B*), *B. thetaiotaomicron* VPI 5492 (*C*), *B. uniformis* ATCC 8492 (*D*), *P. gingivalis* ATCC 33277 (*E*), and *P. distasonis* ATCC 8503 (*F*). Note that the *O*-glycosylation information of *F* is not encoded at a single locus. *Wzx* (*gray*), flippase (found in all species except for *P. gingivalis*); *X* (*green*), UDP-GlcNAc 2-epimerase; *Y* (*pink*), acetyltransferase; *GTi*, *GTii*, and *GTiii* (*blue*), glycoyltransferases. *E* values of $<10^{-5}$ were considered.

[4] G. Sekot, G. Posch, O. Yoojin, S. Zayni, H. F. Mayer, D. Pum, P. Messner, P. Hinterdorfer, and C. Schäffer, unpublished observations.

that the terminal Pse5Am7Gc residue participates in the bacterium-host cross-talk, albeit the relevance of the modification of the pseudaminic acid would currently remain unclear. This is supported by the fact that members of this class of sialic acid-like sugars have been found in many Gram-negative bacterial species as constituents of important cell surface glycoconjugates, such as LPS (42), capsules (43), pili (44), and flagella (45, 46), all of which are important to pathogenicity, possibly influencing bacterial adhesion, invasion, and immune evasion (47). It is tempting to speculate that the glycans are recognized by lectin-like receptors that may mediate adhesion to and invasion of specific host cells (13). It is interesting to note that, recently, for *T. forsythia* a novel sialic acid utilization and uptake system has been described (48), leaving open the principal opportunity of utilization of this sugar as a precursor for Pse5Am7Gc biosynthesis.

Crucial for the overall virulence potential of *T. forsythia* is its specific biofilm life style. Thus, the knowledge of factors triggering biofilm formation might reveal valuable strategies for interfering with periodontal disease. Despite the fact that *T. forsythia* is a so-called second colonizer intercalating with other species from the oral microflora in dental plaque biofilms (49), which is consistent with a polymicrobial disease etiology (10), investigation of monospecies biofilms may also shed light onto factors affecting this specific life style. Thus, we included in our study an isogenic *T. forsythia wecC* mutant, for which increased static monospecies biofilm formation has been observed (6). This was explained by a measured increase in cell surface hydrophobicity, which would promote bacterial attachment and/or aggregation (6). Surprisingly, increased biofilm formation could be correlated with the presence of truncated S-layer glycans on the *T. forsythia*, in which the 4-Me-β-Man*p*NAc-$CONH_2$-(1→3)-[Pse5Am7Gc-(2→4)-]-β-Man*p*NAcA-(1→4)-trisaccharide branch is missing (compare with Fig. 2). Considering a p*K* value of sialic acids of ~2.6, it is evident that under physiological conditions of the basic saliva environment in the oral cavity, the acid functions of these residues are dissociated and, thus, contribute to charge repulsive forces that impair biofilm formation. The finding that there is a negative correlation between *wecC* transcription and biofilm formation (6) supports this assumption. However, currently, it cannot be ruled out that WecC is not the sole cause for S-layer glycan truncation and, consequently, promotion of biofilm formation, because it might well be that the insertional inactivation strategy of *wecC* causes polar effects on downstream genes. If the biological observations with the *wecC* mutant are due solely to the truncated S-layer glycans or if WecC also influences the predicted *T. forsythia* exopolysaccharide as previously believed (6) remains to be investigated.

In the context of biofilm formation, it is interesting to note that besides the *T. forsythia* S-layer glycoproteins, the two glycoproteins TF1259 and TF2339 that have been characterized in the course of the present study are up-regulated in biofilm formation (50). This is a further indication that the S-layer protein *O*-glycosylation system is linked with the biofilm life style of *T. forsythia*.

The finding that several abundant proteins in *T. forsythia* are modified with the S-layer glycan is fueled by the recent identification of a rich outer membrane glycoproteome in *T. forsythia* (34). Our data corroborate and extend a recent study by Veith *et al.* (34), in which all except the TF0091 protein have been already identified as glycoproteins. Notably, there was no information published about the identity of the glycan structure. All of these glycoproteins are antigenic upon probing with an antiserum raised against a *T. forsythia* outer membrane preparation (34). Interestingly, most of the prevalent *T. forsythia* glycoproteins identified in this study (the two S-layer glycoproteins TfsA (TF2261-2262) and TfsB (TF2663), TF2339, and its paralog TF1259) are located in the outer membrane of the bacterium, whereas the others (TF1056 and TF0091) are predicted lipoproteins. TF1259 and TF2339 exhibit C-terminal sequence similarity to the CTD family of *P. gingivalis* (51). TF1056 and TF0091 are predicted non-CTD lipoproteins, showing similarity to TonB-dependent receptor-associated proteins, which are generally known to be important for signal transmission to the cytoplasm and activation of target gene transcription (52).

Overall, the presented data indicate that the periodontal pathogen *T. forsythia* possesses a general protein *O*-glycosylation pathway that modifies proteins of yet undefined function at multiple sites with a complex oligosaccharide within the (D)(S/T)(A/I/L/M/T/V) amino acid motif. The underlying glycosylation machinery as well as the glycosylation "sequon" seems to be conserved within *Bacteriodetes* species. This provokes speculation about the presence of comparable glycosylation patterns, at least in the compared species (compare with Fig. 6). The aspects in which protein *O*-glycosylation is involved in underpinning the pathogenic strategy of *T. forsythia* and in its interaction with other bacteria from the oral microflora will be investigated in future studies.

Acknowledgments—We greatly appreciate the gift of the S-layer gene mutants, T. forsythia ATCC 43037 ΔtfsA and ΔtfsB, from Yukitaka Murakami (Aichi-Gakuin University Nagoya, Japan) and of the UDP-N-acetyl-D-mannosaminuronic acid dehydrogenase mutant T. forsythia ATCC 43037 ΔwecC from Ashu Sharma (State University of New York at Buffalo). We also thank Edeltraud Thiry and Andreas Roitinger (Thermo Fisher Scientific, Bremen, Germany) for performing experiments on the LTQ Orbitrap Velos mass spectrometer. We thank Hanspeter Kählig and Susanne Felsinger (both from the University of Vienna) for diffusion measurements and support with recording the NMR spectra, respectively.

REFERENCES

1. Vik, A., Aas, F. E., Anonsen, J. H., Bilsborough, S, Schneider, A., Egge-Jacobsen, W., and Koomey, M. (2009) *Proc. Natl. Acad. Sci. U.S.A.* **106,** 4447–4452
2. Szymanski, C. M., and Wren, B. W. (2005) *Nat. Rev. Microbiol.* **3,** 225–237
3. Fletcher, C. M., Coyne, M. J., Villa, O. F., Chatzidaki-Livanis, M., and Comstock, L. E. (2009) *Cell* **137,** 321–331
4. DiGiandomenico, A., Matewish, M. J., Bisaillon, A., Stehle, J. R., Lam, J. S., and Castric, P. (2002) *Mol. Microbiol.* **46,** 519–530
5. Byrd, M. S., Sadovskaya, I., Vinogradov, E., Lu, H., Sprinkle, A. B., Richardson, S. H., Ma, L., Ralston, B., Parsek, M. R., Anderson, E. M., Lam, J. S., and Wozniak, D. J. (2009) *Mol. Microbiol.* **73,** 622–638
6. Honma, K., Inagaki, S., Okuda, K., Kuramitsu, H. K., and Sharma, A. (2007) *Microb. Pathog.* **42,** 156–166
7. Socransky, S. S., Haffajee, A. D., Cugini, M. A., Smith, C., and Kent, R. L., Jr. (1998) *J. Clin. Periodontol.* **25,** 134–144

8. Beck, J. D., Slade, G., and Offenbacher, S. (2000) *Periodontol. 2000* **23,** 110–120
9. Li, X., Kolltveit, K. M., Tronstad, L., and Olsen, I. (2000) *Clin. Microbiol. Rev.* **13,** 547–558
10. Sharma, A. (2010) *Periodontol. 2000* **54,** 106–116
11. Sharma, A., Sojar, H. T., Glurich, I., Honma, K., Kuramitsu, H. K., and Genco, R. J. (1998) *Infect. Immun.* **66,** 5703–5710
12. Sabet, M., Lee, S. W., Nauman, R. K., Sims, T., and Um, H. S. (2003) *Microbiology* **149,** 3617–3627
13. Sakakibara, J., Nagano, K., Murakami, Y., Higuchi, N., Nakamura, H., Shimozato, K., and Yoshimura, F. (2007) *Microbiology* **153,** 866–876
14. Sekot, G., Posch, G., Messner, P., Matejka, M., Rausch-Fan, X., Andrukhov, O., and Schäffer, C. (2011) *J. Dent. Res.* **90,** 109–114
15. Sleytr, U. B., Sára, M., Pum, D., Schuster, B., Messner, P., and Schäffer, C. (2002) in *Biopolymers*, Vol. 7 (Steinbüchel, A., and Fahnestock, S., eds) pp. 285–338, Wiley-VCH, Weinheim, Germany
16. Messner, P., Steiner, K., Zarschler, K., and Schäffer, C. (2008) *Carbohydr. Res.* **343,** 1934–1951
17. Ristl, R., Steiner, K., Zarschler, K., Zayni, S., Messner, P., and Schäffer, C. (2011) *Int. J. Microbiol.* **2011,** Article ID 127870
18. Lee, S. W., Sabet, M., Um, H. S., Yang, J., Kim, H. C., and Zhu, W. (2006) *Gene* **371,** 102–111
19. Fletcher, C. M., Coyne, M. J., Bentley, D. L., Villa, O. F., Comstock, L. E. (2007) *Proc. Natl. Acad. Sci. U.S.A.* **104,** 2413–2418
20. Laemmli, U. K. (1970) *Nature* **227,** 680–685
21. Hart, C., Schulenberg, B., Steinberg, T. H., Leung, W. Y., and Patton, W. F. (2003) *Electrophoresis* **24,** 588–598
22. Steiner, K., Novotny, R., Patel, K., Vinogradov, E., Whitfield, C., Valvano, M. A., Messner, P., and Schäffer, C. (2007) *J. Bacteriol.* **189,** 2590–2598
23. Zarschler, K., Janesch, B., Pabst, M., Altmann, F., Messner, P., and Schäffer, C. (2010) *Glycobiology* **20,** 787–798
24. Taylor, A. M., Holst, O., and Thomas-Oates, J. T. (2006) *Proteomics* **6,** 2936–2346
25. Pabst, M., Kolarich, D., Pöltl, G., Dalik, T., Lubec, G., Hofinger, A., and Altmann, F. (2009) *Anal. Biochem.* **384,** 263–273
26. Packer, N. H., Lawson, M. A., Jardine, D. R., and Redmond, J. W. (1998) *Glycoconj. J.* **15,** 737–747
27. Pabst, M., and Altmann, F. (2008) *Anal. Chem.* **80,** 7534–7542
28. Stadlmann, J., Pabst, M., Kolarich, D., Kunert, R., and Altmann, F. (2008) *Proteomics* **8,** 2858–2871
29. Huang, Y., Mechref, Y., and Novotny M. V. (2001) *Anal. Chem.* **73,** 6063–6069
30. Anumula, K. R. (1994) *Anal. Biochem.* **220,** 275–283
31. Chai, W., Feizi, T., Yuen, C. T., and Lawson, A. M. (1997) *Glycobiology* **7,** 861–872
32. Zeleny, R., Kolarich, D., Strasser, R., and Altmann, F. (2006) *Planta* **224,** 222–227
33. Pabst, M., Bondili, J. S., Stadlmann, J., Mach, L., and Altmann F. (2007) *Anal. Chem.* **79,** 5051–5057
34. Veith, P. D., O'Brien-Simpson, N. M., Tan, Y., Djatmiko, D. C., Dashper, S. G., and Reynolds, E. C. (2009) *J. Proteome Res.* **8,** 4279–4292
35. Schäffer, C., Dietrich, K., Unger, B., Scheberl, A., Rainey, F. A., Kählig, H., and Messner P. (2000) *Eur. J. Biochem.* **267,** 5482–5492
36. Wu, D., Chen, A., and Johnson, C. S. Jr. (1995) *J. Magn. Reson. A* **115,** 260–264
37. Pabst, M., Wu, S. Q., Grass, J., Kolb, A., Chiari, C., Viernstein, H., Unger, F. M., Altmann, F., and Toegel, S. (2010) *Carbohydr. Res.* **345,** 1389–1393
38. Steindl, C., Schäffer, C., Smrecki, V., Messner, P., and Müller, N. (2005) *Carbohydr. Res.* **340,** 2290–2296
39. Wang, L., Yin, Z. Q., Wang, Y., Zhang, X. Q., Li, Y. L., Ye, W. C. (2010) *Planta Med.* **76,** 909–915
40. Petersen, B. O., Sára, M., Mader, C., Mayer, H. F., Sleytr, U. B., Pabst, M., Puchberger, M., Krause, E., Hofinger, A., Duus, J. Ø., and Kosma, P. (2008) *Carbohydr. Res.* **343,** 1346–1358
41. Calo, D., Eilam, Y., Lichtenstein, R. G., and Eichler, J. (2010) *Appl. Environ. Microbiol.* **76,** 5684–5692
42. Knirel, Y. A., Shashkov, A. S., Tsvetkov, Y. E., Jansson, P. E., and Zähringer, U. (2003) *Adv. Carbohydr. Chem. Biochem.* **58,** 371–417
43. Kiss, E., Kereszt, A., Barta, F., Stephens, S., Reuhs, B. L., Kondorosi, A., and Putnoky, P. (2001) *Mol. Plant Microbe Interact.* **14,** 1395–1403
44. Castric, P., Cassels, F. J., and Carlson, R. W. (2001) *J. Biol. Chem.* **276,** 26479–26485
45. Thibault, P., Logan, S. M., Kelly, J. F., Brisson, J. R., Ewing, C. P., Trust, T. J., and Guerry, P. (2001) *J. Biol. Chem.* **276,** 34862–34870
46. Schoenhofen, I. C., McNally, D. J., Brisson, J. R., and Logan, S. M. (2006) *Glycobiology* **16,** 8C–14C
47. Hsu, K. L., Pilobello, K. T., Mahal, L. K. (2006) *Nat. Chem. Biol.* **2,** 153–157
48. Roy, S., Douglas, C. W., and Stafford, G. P. (2010) *J. Bacteriol.* **192,** 2285–2293
49. Marsh, P. D., Moter, A., and Devine, D. A. (2011) *Periodontol. 2000* **55,** 16–35
50. Pham, T. K., Roy, S., Noirel, J., Douglas, I., Wright, P. C., and Stafford, G. P. (2010) *Proteomics* **10,** 3130–3141
51. Veith, P. D., Talbo, G. H., Slakeski, N., Dashper, S. G., Moore, C., Paolini, R. A., Reynolds, E. C. (2002) *Biochem. J.* **363,** 105–115
52. Koebnik, R. (2005) *Trends Microbiol.* **13,** 343–347
53. Wuhrer, M., Deelder, A. M., and van der Burgt, Y. E. (2011) *Mass Spectrom. Rev.* **30,** 664–680